IMPACT OF THE MODULATED ANNUAL CYCLE AND THE INTRASEASONAL OSCILLATION ON DAILY-TO-INTERANNUAL RAINFALL VARIABILITY ACROSS MONSOONAL INDIA

Vincent MORON (+,*), Andrew W. ROBERTSON (*) Michael GHIL (++, **)

(+) Aix-Marseille University & CEREGE, Aix-en-Provence, France, and Institut Universitaire de France, Paris, France - (e-mail: V.M. : moron@cerege.fr)
(*) International Research Institute for Climate and Society (IRI), The Earth Institute, Columbia University, Palisades, NY, USA - (e-mail: A.W.R. : awr@iri.columbia.edu)
(++) Department of Atmospheric & Oceanic Sciences and Institute of Geophysics & Planetary Physics, University of California, Los Angeles, CA 90095-1565, USA
(**) Geosciences Department and Laboratoire de Météorologie Dynamique (CNRS and IPSL), École Normale Supérieure, Paris, France - (e-mail: M.G. : ghil@lmd.ens.fr)

1 INTRODUCTION & GOALS

The goal of this poster is to revisit the question of intraseasonal-to-interannual variability of the Indian summer monsoon, using a framework that allows the intraseasonal (ISO) and interannual modulations of the monsoon's seasonal cycle to be treated in a unified oscillatory way, and without the need for explicit pre-filtering of the data.

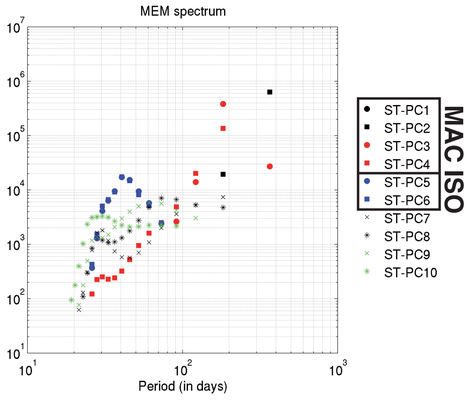

Figure 1: Power spectra of the ten leading space-time principal components (ST-PCs) from multichannel singular spectrum analysis (M-SSA) of daily outgoing long-wave radiation (OLR) and zonal and meridional components of the 925-hPa winds. The spectra were computed separately for each ST-PC by using the maximum entropy method with a 60-day window over Monsoonal India (60°–100°E, 0–35°N); the legend in the figure gives the key to individual-PC results. The missing period from March 17 to December 31, 1978, in the OLR data set is replaced with the OLR mean seasonal cycle computed on the available data. Mean and standard deviations are computed for the whole available period and used to normalize the anomalies. An empirical orthogonal function (EOF) analysis is then applied to the standardized anomalies of OLR and wind to retain 75% of the entire variance, which yields the 26 leading principal components (ordinary, spatial-only PCs). Solely spectral peaks that are significant according to a Monte Carlo test with 1000 realizations of an auto-regressive process of order one (AR1 or "red noise") are displayed.

2 EXTRACTION OF MODULATED ANNUAL CYCLE AND INTRASEASONAL OSCILLATION USING M-SSA

- Multichannel Singular Spectrum Analysis (M-SSA) with a window width M = 60 days is applied to unfiltered OLR, together with the zonal and meridional components of the wind at 925 hPa (60°-100°E, eq.-35°N).
- The M-SSA components 1–4 capture the annual cycle, while pair 5-6 represents intraseasonal oscillation (ISO) (**Fig. 1**). The sum of reconstructed components 1-4 is referred to hereafter as the "modulated annual cycle" (MAC), because their phase and amplitude are modulated from year to year.
- Reconstructions of the zonally averaged OLR associated with the MAC and ISO are illustrated in **Fig. 2** for the year 1987 (a "bad" monsoon year). The seasonal variation is clearly isolated by the MAC (**Fig. 2b**), together with the striking temporal asymmetry of the abrupt onset and smoother retreat of the summer monsoon. The ISO (**Fig. 2c**) is active from May to December, with a clear northward propagation that is visible even in the raw data (**Fig. 2a**).
- The phase composites of the MAC (**Fig. 3**) exhibit a predominantly standing-wave, north-south pattern, with little spatial phase propagation, as seen already in **Fig. 2b**.
- The phase composites of the ISO (**Fig. 4**) are characterized by a northward propagation of OLR anomalies, with a strongly reduced amplitude north of about 20°N.

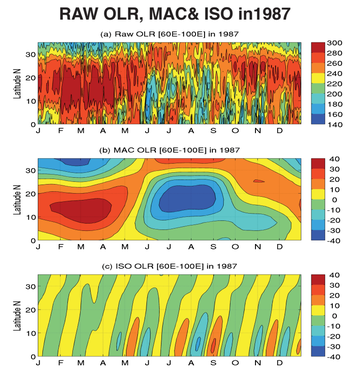

Figure 2: Time-latitude diagram of the longitudinal mean (60°–100°E) for the dry year 1987 of (a) daily OLR (in Wm-2); (b) MAC (RCs 1–4); and (c) ISO (RCs 5-6) from the M-SSA reported in Fig. 1. Units in panels (b) and (c) are anomaly (in Wm-2) relative to the long-term mean.

3 PHASE COMPOSITE OF THE MAC

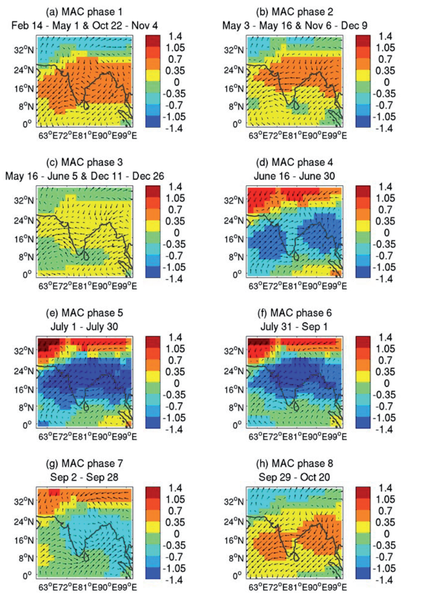

Figure 3: Phase composites of the MAC; OLR standardized anomalies shown as shadings and standardized anomalies of the zonal and meridional components of the 925-hPa winds shown as vectors. The eight phases are computed relative to the spatial average of MAC OLR over Monsoonal India (Gadgil, 2003).

4 PHASE COMPOSITE OF THE ISO

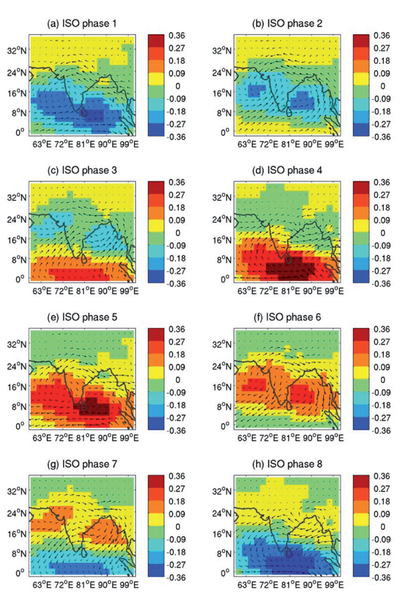

Figure 4: Same as **Fig. 3**, but for the ISO. The eight phases are computed from the ISO average of the ISO OLR over Monsoonal India.

5 HMM STATES OF DAILY RAINFALL

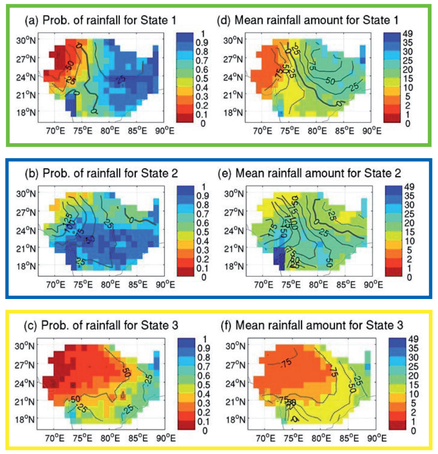

Figure 5: Characteristics of the three Hidden Markov Model (HMM) states obtained, during wet days: (a–c; left column) probability (shadings) and probability anomaly in % (contours); and (d–f, right column) mean rainfall (shadings) and mean rainfall anomaly in % (contours); computed from daily rainfall during JJAS for the full data set (1975–2008) across Monsoonal India.

6 VITERBI SEQUENCE OF HMM STATES

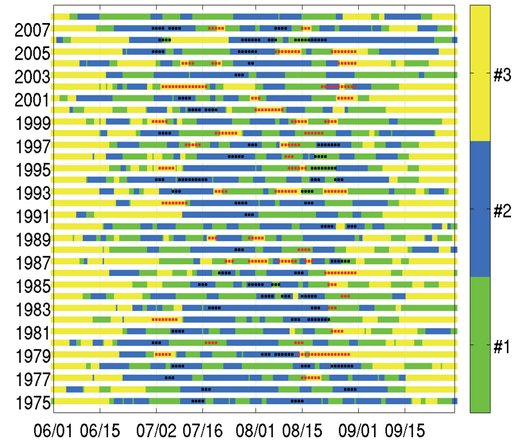

Figure 6: Viterbi sequence of the three hidden Markov model (HMM) states with "active" and "break" days superimposed as black and red squares respectively from Rajeevan et al. (2008). State 1 is shown as green squares , State 2 as blue squares, and State 3 as yellow squares; the active and break days documented by Rajeevan et al. (2008) are shown as black and red dots, respectively.

7 HMM STATE VS MAC & ISO

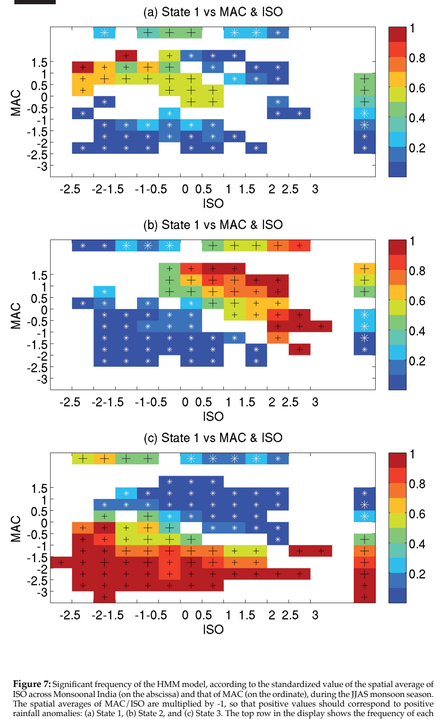

Figure 7: Significant frequency of the HMM model, according to the standardized value of the spatial average of ISO across Monsoonal India (on the abscissa) and that of MAC (on the ordinate), during the JJAS monsoon season. The spatial averages of MAC/ISO are multiplied by -1, so that positive values should correspond to positive rainfall anomalies: (a) State 1, (b) State 2, and (c) State 3. The top row in the display shows the frequency of each HMM state according to the standardized value of the spatial average of ISO across Monsoonal India, while the rightmost column corresponds to that given by the marginal MAC distribution. The black plus sign indicates significant positive anomalies at the two-sided 90% level, according to a Monte Carlo test based on reshuffling the Viterbi sequence 1000 times (see text for details), while the white asterisks are for significant negative anomalies; the larger symbols indicate an absolute number of occurrences of at least 30 days.

8 HMM STATES & MAC FOR WET AND DRY YEARS

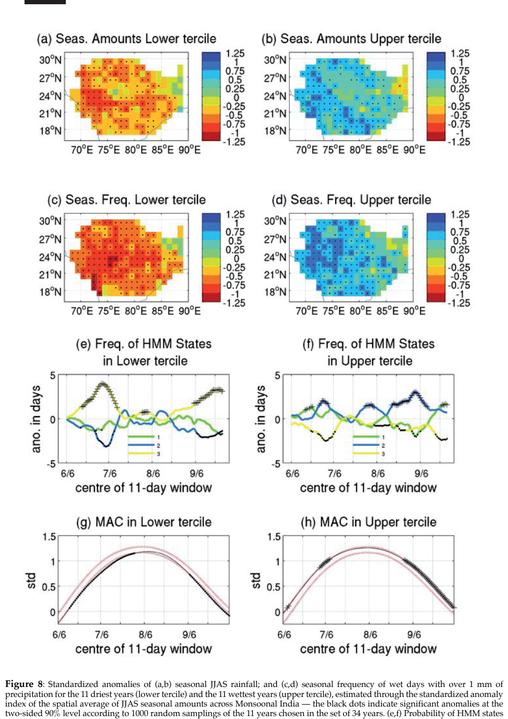

Figure 8: Standardized anomalies of (a,b) seasonal JJAS rainfall; and (c,d) seasonal frequency of wet days with over 1 mm of precipitation for the 11 driest years (lower tercile) and the 11 wettest years (upper tercile), estimated through the standardized anomaly index of the spatial average of JJAS seasonal amounts across Monsoonal India — the black dots indicate significant anomalies at the two-sided 90% level according to 1000 random samplings of the 11 years chosen in the set of 34 years. (e,f) Probability of HMM states over 11-day sliding windows for lower- and upper-tercile years, expressed as deviation in days with respect to the long-term mean; the plus signs and dots indicate positive and negative anomalies, respectively, which are significant at the two-sided 90% level, according to 1000 random permutations of the Viterbi sequence, while the color convention for the three states is the same as in Figs. 9 and 11. (g,h) Mean daily value of MAC OLR for lower and upper terciles (black line) with the 90% confidence interval from 1000 samples of 11 years randomly chosen in the set of 34 years; plus signs and dots as in panels (e,f).

INTRASEASONAL AND INTERANNUAL RELATIONSHIPS BETWEEN MAC/ISO AND DAILY RAINFALL ACROSS MONSOONAL INDIA

- HMM state 1 = east-west dipolar pattern (**Figs. 5a,d**).
- HMM state 2 = wet almost everywhere, especially south of about 24°N, with relatively drier conditions further north (**Figs. 5b,e**).
- HMM state 3 = dry almost everywhere, except in the northeast corner of the domain, near Assam (**Figs. 5c,f**).
- Interannual variability of spatially averaged JJAS rainfall across Monsoonal India is strongly correlated with the frequencies of occurrence for State 2 ($r = 0.83$, sig. > 99%) and State 3 ($r = -0.87$, sig. > 99%), but not with State 1 ($r = 0.12$, sig. < 75%).
- State 3 (yellow squares in the figure 6) is naturally more prevalent in June and September, before and after the core of the monsoon, but also occurs in short spells during July–August in some years (e.g. in 1987, 1993, and 2002). States 1 (green squares) and 2 (blue squares) are concentrated in July–August without any clear temporal preference. The 252 break days from Rajeevan et al. (2008) fall mostly into State 1 (86 days) and state 3 (157 days), with the remaining 9 classified as State 2 (**Fig. 6**).
- The occurrence of the dry State 3 (**Fig. 7c**) is largely controlled by MAC. The impact of ISO on State 3 becomes significant when MAC is between −1 and 0.5, with positive ISO favoring fewer State-3 occurrences.
- The interaction between MAC and ISO is more substantial for the wet State 2 that coincides with active spells of the monsoon. The marginal MAC and ISO distributions are more similar in this case, and there is a systematic tendency for low State-2 probabilities when MAC and ISO values are negative, and toward high State-2 probabilities when MAC and ISO values are positive (**Fig. 7b**).
- The dependence of State 1, with its west-east dipolar rainfall, on ISO is the least pronounced, which is consistent with the large longitudinal scale of the ISO. State 1 is favored when MAC is positive, e.g., during the core of the summer monsoon, as apparent also from the Viterbi state sequence.
- Driest years = higher prevalence of the dry State 3 and less of the wet State 2 from mid-June to early July, and then again in September (**Fig. 8e**). The tendency toward more breaks (State 3) during the core of the monsoon season is nonetheless significant (for example in 1987, 1993, 2000 and 2002).
- Wettest years = lower prevalence of the dry State 3, especially from mid-June to early July, and then from August onward, and higher prevalence of the wet State 2 around the end of June, late July, and most prominant from late August onward (**Fig. 8e**).
- The main significant changes in state frequency occur near the onset and end of the monsoon season, with consistent departures seen in the wet and dry states (States 1 and 3), while broad-scale rainfall anomalies during the core of the monsoon season are less marked in state frequency.
- The amplitude of the MAC shows consistent deviations between the two sets of years (**Figs. 8g,h**), especially from mid-June to late-July and then in September, although the deviations do not always exceed the 90% significance level, as computed from 1000 randomly chosen sets of 11 years each. Thus, both the MAC as well as the deviations in state frequency and suggest that JJAS seasonal anomalies across Monsoonal India are predominantly due to the changes in the length of the monsoon season.

Concluding remarks

- The MAC (**Fig. 3**) and ISO (**Fig. 4**) are shown to represent the dominant components of atmospheric circulation variability over India.
- A three-state hidden Markov model characterized by rainfall patterns that are "dry" (State 3), "wet" (State 2), and "wet-in-the-east" (State 1) (**Fig. 5**) provides a useful minimal description of the main attributes of the seasonal cycle, as well as of the active and break monsoon episodes (**Fig. 6**) that were identified in previous studies.
- The occurrence of rainfall States 3 and, especially, 2 is shown to be a strong function of the combined MAC and ISO effects, despite the relatively small amplitude of the latter (**Fig. 7**). Thus, positive anomalies of both MAC and ISO accompany more frequent occurrence of active phases of the monsoon, while negative anomalies of the two oscillatory components are associated with the break phases. Finally, the role of ISO is stronger for near-neutral values of MAC. Even though State 1 appears to be less controlled by the combination of MAC and ISO, its occurrence is more frequent when the eastern cyclonic anomaly nears the Bay and Bengal (**Fig. 4**, Phases 4-5). In this context, it could follow State 2, which occurs mostly when the near-zonal anomalous trough is close to 18°–22°N (**Fig. 4**, Phases 2-3).
- Still, the weak negative relationship between ISO seasonal amplitude and the SAI of JJAS rainfall amounts results from a relatively strong asymmetric relationship. The first source of asymmetry lies in the seasonal modulation of the MAC–ISO interaction and its impact on state occurrence, as just mentioned above (**Fig. 7**), and also in the fact that these features appear to exhibit noticeable asymmetry between anomalously dry and wet seasons. Another source of asymmetry is spatial: the strongest anomalies of JJAS rainfall amounts during dry and wet years are modulated in space, with a stronger signal in the southern and western parts of Monsoonal India (**Fig. 8**). We need to be cautious here about potential sampling uncertainty, since the analyzed time interval is rather short but the asymmetry could also be due to the actual evolution of ISO itself (**Fig. 4**). The fact that the ISO itself is symmetric about zero does not necessarily lead to seasonally averaged anomalies being vanishingly small, because of the interaction with the MAC. For example, a weak MAC would bolster the role of the "anticyclonic" phase — with more breaks, less active spells or both — vs. the "cyclonic" phase of the oscillation.
- Finally, it seems worth mentioning that M-SSA, in combination with the maximum entropy method (recall **Fig. 1** here) could lead to highly competitive prediction skill of those features of the phenomena analyzed here that do capture substantial variance of the rainfall amounts or frequencies. Indeed, this combination has been proven to be quite successful in predicting certain features of the El Niño–Southern Oscillation phenomenon in the Eastern Tropical Pacific. We expect that similar success could be encountered in this context, especially when combining this spectral approach for the large-scale features with the HMM one used in characterizing the rainfall states.

Acknowledgments. We are grateful to M. Rajeevan and the India Meteorological Department for supplying the Indian rainfall data set. Interpolated OLR data were provided by the Physical Sciences Division (PSD) of the Earth System Research Laboratory (ESRL) of the National Oceanic and Atmospheric Administration (NOAA), in Boulder, Colorado, USA, from their Web site at http://www.esrl.noaa.gov/psd/data/gridded/data.interp_OLR.html. The NHMM software (MVNHMM) was developed by S. Kirshner and can be obtained free of charge from http://www.stat.purdue.edu/~skirshne/MVNHMM/. This research was supported by grant NA050AR4311004 from the National Oceanic and Atmospheric Administration (NOAA) to Columbia University (AWR) and by the Department of Energy's grant DE-FG02-07ER64439 from its Regional and Global Climate Modeling (RGCM) Program to UCLA (MG). Interaction between the authors was facilitated by a grant from the Institut Universitaire de France to VM.